Rapid state-dependent alteration in K$_v$3 channel availability drives flexible synaptic signaling dependent on somatic subthreshold depolarization

Matthew J.M. Rowan[1] and **Jason M. Christie**[1,*]

[1]Max Planck Florida Institute for Neuroscience, Jupiter, FL USA

Summary

In many neurons, subthreshold depolarization in the soma can transiently increase action potential (AP)-evoked neurotransmission via analog-to-digital facilitation. The mechanisms underlying this form of short-term synaptic plasticity are unclear, in part, due to the relative inaccessibility of the axon to direct physiological interrogation. Using voltage imaging and patch-clamp recording from presynaptic boutons of cerebellar stellate interneurons, we observed that depolarizing somatic potentials readily spread into the axon, resulting in AP broadening, increased spike-evoked Ca^{2+} entry, and enhanced neurotransmission strength. K$_v$3 channels, which drive AP repolarization, rapidly inactivated upon incorporation of K$_v$3.4 subunits. This leads to fast susceptibility to depolarization-induced spike broadening and analog facilitation independent of Ca^{2+}-dependent protein kinase C signaling. The spread of depolarization into the axon was attenuated by hyperpolarization-activated currents (I$_h$) in the maturing cerebellum, precluding analog facilitation. These results suggest that analog-to-digital facilitation is tempered by development or experience in stellate cells.

Graphical abstract

Address for Correspondence: Jason M. Christie, Max Planck Florida Institute for Neuroscience, Jupiter, FL USA, jason.christie@mpfi.org.
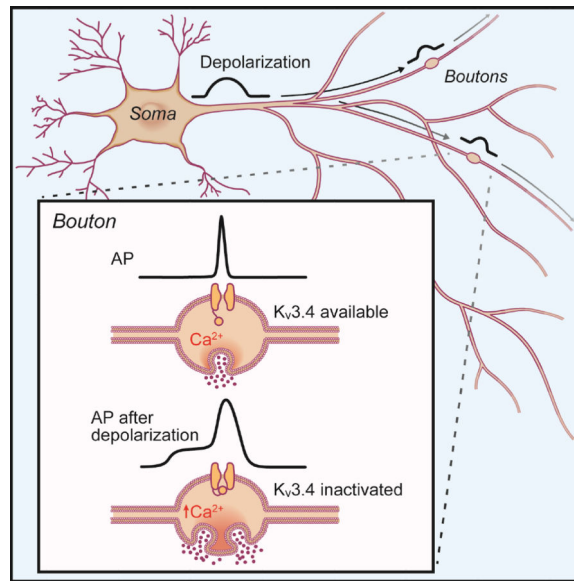*Lead Contact

Introduction

Short-term synaptic plasticity enriches the signaling capacity of a neural circuit endowing interconnected neurons greater flexibility in information processing (Abbott and Regehr, 2004). Although short-term plasticity is known to result from use-dependent activity during repetitive spiking (Zucker and Regehr, 2002), recent evidence indicates that the strength of neurotransmission may also be subject to modulation by depolarizing potentials below threshold for spike initiation. Due to strong electrotonic coupling in many cell types, somatic subthreshold depolarization can spread into the axon reaching distant presynaptic specializations and transiently increasing AP-evoked synaptic transmission (Alle and Geiger, 2006; Shu et al., 2006). This form of short-term plasticity is generally understood to result from inactivation of K_v1-type channels during prolonged depolarization of the axon initial segment (Kole et al., 2007) or more distal axon locations (Bialowas et al., 2015; Foust et al., 2011; Shu et al., 2006; Zhu et al., 2011) leading to broadening of subsequent APs thus increasing spike-evoked neurotransmission at sites of release. However, synaptic depolarization also results in Ca^{2+}-dependent enhancement of vesicular priming (Awatramani et al., 2005) and exocytosis (Christie et al., 2011) that may deplete the readily releasable pool. Whether these distinct mechanisms act in combination to modify AP-evoked release is unclear (Rama et al., 2015).

In the cerebellum, GABA-releasing stellate cell (SC) interneurons are subject to analog control of neurotransmission. Depolarizing potentials that invade the SC axon increase residual Ca^{2+} and can drive asynchronous vesicular fusion (Bouhours et al., 2011; Christie et al., 2011; Glitsch and Marty, 1999). Somatic depolarization also increases AP-evoked Ca^{2+} entry (Christie et al., 2011; but see Bouhours et al., 2011) suggesting that AP duration may be subject to modulation in SC boutons. In the axons of excitatory neocortical and hippocampal cells, activity-dependent modification of AP duration is mediated through changes in K_v1 channel availability through slow accumulation of inactivation including

during subthreshold depolarization (Bialowas et al., 2015; Kole et al., 2007; Shu et al., 2006). However AP duration is controlled primarily by K_v3-type channels at SC boutons, similar to other inhibitory interneurons (Rowan et al., 2016). Thus AP broadening in SC axons likely involves K_v3 channel modulation but, paradoxically, K_v3 channels are thought to be essential for maintaining AP waveform fidelity (Lien and Jonas, 2003; Whim and Kaczmarek, 1998). Interestingly, the extremely fast adaptive properties of inactivating K_v3 subunits (Baranauskas et al., 2003) may confer a mechanism for ultra-rapid analog modulation of neurotransmission required for many network computations. Whether K_v3 channels contribute to activity-dependent plasticity during analog signaling is currently unknown.

We used two-photon (2P) voltage-sensitive dye imaging and direct bouton patch-clamp recording to examine the mechanisms contributing to analog signaling in SC axons. We find that brief subthreshold somatic potentials spread throughout a large extent of the axon arbor, transiently inactivating $K_v3.4$ subunit-containing K_v3 channels that drive AP repolarization thus increasing the width of subsequent spikes. Spike broadening increases AP-evoked Ca^{2+} influx accounting for the analog enhancement of AP-evoked release. In the absence of AP broadening, somatic depolarization induces rapid synaptic depression suggesting interplay between opposing plasticity mechanisms to determine the effect of subthreshold activity on the strength of neurotransmission. Together, our findings indicate that rapidly inactivating K_v3 currents at sites of release allow for greater flexibility in activity-dependent modulation of neurotransmission multiplying the computational capacity of these neural elements.

Results

Subthreshold somatic depolarization invades the axon

We used voltage-sensitive dye (VSD) imaging to directly measure the extent to which subthreshold depolarizing potentials invade SC axons of juvenile mice (PND 15–21). Cells were filled with the VSD di-2-AN(F)EPPTEA (Acker et al., 2011) during whole-cell current-clamp recording and, after an equilibration period, fluorescence transients were collected from diffraction-limited points along the axon using non-scanning 2P excitation (Rowan et al., 2014). Depolarizing potentials evoked by current injection in the soma (24.6 ± 0.4 mV) from rest (−72.3 ± 0.3 mV) were resolved as an increase in fluorescence in the axon (Figure 1A and 1B) including locations several hundred microns from the soma indicating significant penetration into the arbor. To quantify voltage attenuation along the axon cable, we referenced the amplitude of the depolarizing potential to the peak of an AP measured at the same location in alternating (0.2 Hz) trials (Figure 1B and 1C). This procedure is necessary because VSDs are not uniformly distributed in the axon precluding direct comparison of peak fluorescence changes from multiple locations within and between cells (Peterka et al., 2011). In a separate set of control measurements at the soma, we ensured that the VSD linearly reported voltage changes across a physiologically relevant range of membrane potentials (Figure 1D). From our axonal VSD measurements, a monoexponential fit to the data points yielded an estimate of the length constant (θ) for subthreshold depolarization (100 ms) of 220 μm. Because SC axons project ~300 μm on

average (de San Martin et al., 2015), this result shows that somatic subthreshold potentials invade a significant portion of the SC axon arbor.

Rapid modulation of AP duration following subthreshold depolarization at boutons

Accumulating evidence indicates that, in axons, spike duration is subject to use-dependent modulation. For example, repetitive spiking can progressively drive spike broadening (Geiger and Jonas, 2000; Kole et al., 2007; Rowan et al., 2014; von Gersdorff and Borst, 2002). Thus, rather than an invariant pulse, AP shape is malleable dependent on the history of preceding activity. To determine whether subthreshold activity at the soma can modify spike duration in the axon, we paired APs with or without preceding somatic depolarization in interleaved trials and measured spikes at presynaptic boutons with VSD imaging. We found that brief somatic depolarization (100 ms) resulted in significant broadening of the presynaptic spike (Figure 2A); an effect also observed at near-physiological temperatures (100 ms at 32°C; $128.0 \pm 13.9\%$ of control AP duration; $p < 0.05$; wilcoxon matched-pairs test; $n = 8$). Axonal spike broadening increased with the duration of somatic depolarization (Figure 2B) showing an initial rapid onset and then progressing more slowly for longer lasting potentials (i.e., >100 ms). Depolarization-induced AP broadening decayed after the subthreshold stimulus ended with spike width recovery occurring after approximately 300 ms (Figure 2C) indicating a short-lived affect. Larger-amplitude somatic potentials were more effective at inducing spike broadening as expected for a voltage-dependent process (Figure 2D). However, we observed a weak correlation between spike broadening and distance from soma (Figure 2E). In contrast to effects on spike duration, AP peak amplitude was unaffected by subthreshold depolarization (Figure 2F). These results indicate that the spike repolarization rate at presynaptic sites of release is subject to ultra-rapid modulation induced by depolarizing potentials emanating from the soma, resulting in a short-term plastic alteration of AP duration.

Interestingly, when recording near the axon initial segment (AIS; 10.1 – 37.4 μm from the axon hillock), we found that AP duration was by unaffected by brief somatic depolarization (25.4 ± 0.7 mV) (Figure S1A). Increasing the duration of the depolarization failed to induce spike broadening in this region (1000 ms depolarization; 113.3 ± 7.9 % of matched control; $p > 0.05$; paired t-test; $n = 5$) indicating that AP duration in the AIS was resistant to rapid change by somatic subthreshold voltage activity. We also examined axon shafts that adjoin boutons for depolarization-induced spike broadening. Although somatic depolarization resulted in broader spikes in this region, the effect was slight and significantly less than that observed in boutons (Figure S1B and S1C). Thus, although somatic depolarization spreads across a large portion the SC axon, subthreshold activity-induced AP plasticity is governed in a compartment-specific manner, restricted largely to release sites.

Depolarization-induced AP broadening depends on K$_V$3 channels

Axons achieve a high degree of specificity in the control of excitability within their compartments dependent, in part, on the organization of ion channels that populate their membrane including K_V channels that direct spike repolarization rate (Debanne et al., 2011). In SCs, fast-activating K_V3 channels are particularly enriched at boutons and are the predominant K_V channel conductance setting spike duration (Laube et al., 1996; Rowan et

al., 2016; Southan and Robertson, 2000). To determine whether K_v3 activity is required for depolarization-induced spike broadening, we measured AP duration in boutons in the presence of low-concentration TEA (500 μM) (Baranauskas et al., 2003; Ishikawa et al., 2003). As previously reported (Rowan et al., 2016; Rowan et al., 2014), TEA induced an increase in basal AP duration in boutons (126.9 ± 5.6 % of control AP duration; n = 9; p < 0.05; paired t-test) indicating loss of K_v3 activity during spiking. Importantly, in this condition, somatic depolarization no longer induced spike broadening (Figure 3A). Using the K_v3 blocker 4AP or the K_v3 modulator BDS-1 (30 or 1 uM, respectively; Alle et al., 2011; Yeung et al., 2005), we obtained a similar result (AP width following depolarization 98.4 ± 5.5% of control; n = 6; p > 0.05; paired t-test). This indicates that the plastic increase in AP duration following subthreshold depolarization was occluded by the functional loss of K_v3 channels. Occlusion was not due to attenuation of axosomatic coupling as we continued to observe spread of somatic depolarization into the axon in the absence of K_v3 current (amplitude of axonal potential in TEA 94.9 ± 22.5 % of control; p > 0.05; n = 5; paired t-test). The average increase in spike width induced by somatic depolarization was similar to that induced pharmacologically in matched examples (AP width 116.0 ± 2.4 and 119.2 ± 5.1% of control by depolarization and K_v3 blockers, respectively; n = 11; p > 0.05; paired t-test), however, analog modulation of spike width at individual bouton sites was not correlated with the width change induced by K_v3 block (p > 0.05; n = 11; Pearson correlation) (Figure 3B). This may be reflective of underlying differences in the K_v3 channels whose density and subunit composition vary amongst presynaptic sites throughout the axon (Rowan et al., 2016).

At SC boutons, K_v3 channels include the constituent subunits $K_v3.1$ and $K_v3.4$ (Rowan et al., 2016). We examined for the contribution of these subunits to depolarization-induced spike broadening using $K_v3.1^{-/-}$ and $K_v3.4^{-/-}$ KO mice. Somatic depolarization (22.1 ± 1.2 mV, 100 ms) increased AP duration in boutons of $K_v3.1^{-/-}$ mice (Figure 3C) similar to that observed in wild-types (WTs) (AP width 119 ± 2.9 % and 117 ± 4.3 % of control, n = 29 and 13; WT and $K_v3.1^{-/-}$ mice, respectively; p > 0.05; unpaired t-test). However, in $K_v3.4^{-/-}$ mice, APs were resistant to modulation following somatic depolarization (Figure 3D) despite spread of the subthreshold potential into the axon with an efficacy comparable to both WTs and $K_v3.1^{-/-}$ mice (Figure 3E). Together, these results show that K_v3-mediated currents are necessary for the expression of depolarization-induced spike plasticity in SC axons and indicate that the unique biophysical features of $K_v3.4$ subunits underlie susceptibility to AP modulation.

Inactivating properties of K_v3 currents at boutons

We used axon-attached patch recording to characterize the response profile of pharmacologically-isolated K_v3 currents in SC boutons (Figure 4A). In WT mice, maximally depolarizing pulses (+50 mV; 200 ms) evoked fast-activating currents that showed transient inactivation (Figure 4B). Exponential fits to evoked currents yielded an average decay constant of t = 184 ± 69 ms. However, decay times varied considerably between recording sites (range 4 –489 ms; Figure 4D) indicating that inactivation rate is likely a heterogeneous feature of K_v3 currents across boutons perhaps related to differences in the subunit composition of channels at each particular bouton location. Notably,

inactivation was apparent at hyperpolarized membrane potentials (-50 mV; $\tau = 122 \pm 106$ ms; n = 5; Figure 4C) below the threshold for somatic spike initiation (-39.5 ± 0.5 mV; n = 5). This shows that the availability of K_v3 current can be influenced by inactivation even at hyperpolarized membrane potentials. In recombinant expression systems, homomeric channels composed of $K_v3.1$ subunits generate delayed-rectifier currents whereas $K_v3.4$-containing channels show rapid A-type inactivation (Baranauskas et al., 2003). In $K_v3.1^{-/-}$ mice, we found that the inactivation rate of K_v3 current was not significantly different than that measured in WT animals (Figure 4B and 4D). However, in $K_v3.4^{-/-}$ mice, rapid inactivation was absent resulting in significant slowing of the current decay constant (Figure 4B and 4D). From these results we conclude that $K_v3.4$-dependent inactivation during subthreshold depolarization results in use-dependent AP broadening explaining spike-width plasticity at SC release sites.

Analog facilitation results from K_v3 inactivation-induced spike plasticity

At presynaptic sites of release, spike repolarization rate is a key parameter determining the amount of Ca^{2+} influx during a spike because the AP is the command waveform directing voltage-gated Ca^{2+} channel (Ca_v) opening (Bischofberger et al., 2002; Geiger and Jonas, 2000). Therefore, it is expected that AP broadening induced by inactivation of K_v3 current at SC boutons underlies depolarization-induced enhancement of AP-evoked Ca^{2+} entry (Christie et al., 2011). We directly examined for this using simultaneous voltage and Ca^{2+} imaging at boutons by including chromatically-compatible VSD and Ca^{2+} indicator dyes in the patch pipette (Rowan et al., 2014). Following somatic depolarization, we observed a significant enhancement of spike-evoked Ca^{2+} entry coincident with spike broadening (peak F/F $110.0 \pm 3.6\%$ of control; $p < 0.05$; paired t-test; n = 7; Figure S2A). Indeed, the increase in AP-evoked Ca^{2+} entry following subthreshold depolarization linearly tracked the change in AP duration (Figure S2B) as expected from kinetic modeling of Ca_v channel gating (Li et al., 2007). Therefore, depolarization-induced spike plasticity results in enhancement of AP-evoked Ca^{2+} entry at sites of release.

By directing Ca^{2+} entry, spike width informs release probability (Borst and Sakmann, 1999; Sabatini and Regehr, 1996) thus the accompanying increase in AP-evoked Ca^{2+} influx following depolarization-induced spike broadening is the most parsimonious mechanistic explanation underlying analog facilitation. To assess this hypothesis, we measured release using presynaptic GABA receptor-mediate autoreceptor (pre-$GABA_AR$) currents. Evoked in voltage-clamp mode following a brief somatic pulse (0.5–1.0 ms; +10 mV), these autoreceptor currents result from unclamped spikes in the axon driving GABA exocytosis and subsequent binding to pre-$GABA_AR$ expressed near the sites of release (Pouzat and Marty, 1999). As previously reported (Bouhours et al., 2011), the amplitude of pre-$GABA_AR$ currents increased following somatic depolarization in WT mice (peak amplitude $120.0 \pm 5.9\%$ of control; 100 ms depolarization to -50 mV; $p < 0.05$; n = 13; paired t-test; Figure 5A). This was accompanied by a reduction in the paired pulse ratio (PPR; Figure 5D) indicating that analog facilitation induced by somatic depolarization results from an increase in release probability.

To determine whether the loss of depolarization-induced spike broadening abrogates analog facilitation, we measured autoreceptor currents in K_v3 subunit KO mice. Although somatic depolarization was effective at driving an increase in pre-$GABA_A$R current amplitude in $K_v3.1^{-/-}$ mice comparable to WTs (Figure 5B-5D), we failed to observe facilitation in $K_v3.4^{-/-}$ mice which lack spike plasticity. Instead, subthreshold somatic depolarization in $K_v3.4^{-/-}$ mice resulted in synaptic depression (peak amplitude 90.9 ± 4.2% of control; p < 0.05; n = 15; paired t-test) and concomitantly increased PPR (Figure 5D) as expected for weakened synapses (Zucker and Regehr, 2002). The amount of synaptic weakening induced by somatic depolarization in $K_v3.4^{-/-}$ mice was correlated with PPR, a measure of basal release probability, as observed in interleaved control trials (Figure 5E). Yet basal PPR did not differ between WT and K_v3 KOs (p > 0.05; 1-way ANOVA followed with Tukey's multiple comparisons) indicating the absence of intrinsic differences in release efficacy in mutant mice. From these results, we conclude that depolarization-induced spike broadening is necessary for analog facilitation in SCs. However, in the absence of $K_v3.4$-dependent spike broadening, analog depression abounds pointing to a competing plasticity processes, likely through vesicle depletion by asynchronous release during the depolarizing stimulus (Christie et al., 2011).

Analog facilitation does not require Ca^{2+}-dependent PKC activation

Residual increases in presynaptic Ca^{2+}, such as those that occur during subthreshold depolarization (Awatramani et al., 2005; Bouhours et al., 2011; Christie et al., 2011), could activate protein kinase C (PKC) resulting in enhancement of release through changes in the readily releasable pool (Fioravante et al., 2011). In fact, blockade of PKC activity has been reported to abolish analog facilitation in SCs (Bouhours et al., 2011) however pharmacological tools to activate or inhibit Ca^{2+}-dependent forms of PCK often lack specificity and selectivity (Brose and Rosenmund, 2002). To assess whether Ca^{2+}-dependent PKC activity is involved in analog facilitation, we used mutant mice deficient for all three classical Ca^{2+}-dependent isoforms of PKC ($PKC\alpha^{-/-}$, $PKC\beta^{-/-}$ and $PKC\gamma^{-/-}$). In triple KO ($PKC_{\alpha\beta\gamma}^{-/-}$) mice, enhancement of the pre-$GABA_A$R current was comparable to that in WT mice (129.6 ± 10.4% of control; p 0.05; n = 17; paired t-test; Figure 6A) and displayed a reduction in PPR (86.9 ± 6.7% of control; p 0.05; n = 17; paired t-test; Figure 6B). Thus, activation of Ca^{2+}-dependent PKC appears unnecessary for analog facilitation in SCs.

Analog signaling is developmentally regulated

Although spread of somatic depolarization has been observed in the axons of several neuron types (Alle and Geiger, 2006; Shu et al., 2006), this is not a universal signaling feature. For example, the axons of CA1 pyramidal cells appear uncoupled from the soma due to active attenuation by a K^+-channel conductance (Apostolides et al., 2016). Surprisingly, in axonal VSD measurements from mature mice (PND 42), we found that subthreshold depolarization (100 ms) spread less readily in SCs compared to juveniles (Figure 7A and 7B). Furthermore, we failed to observe depolarization-induced AP broadening in mature animals (AP width 95.0 ± 2.4% of control; p > 0.05; wilcoxon matched-pairs test; n = 13; Figure 7C), a likely consequence of axonal filtering. Thus it appears that in the mature cerebellum, spike broadening and analog facilitation are not present suggesting the capacity

of SC axons to support these features is subject to regulation following experiential or developmental cues.

A developmental shift in axosomatic coupling may result from alterations in the active properties of the axon. Hyperpolarization-activated cation (HCN) channels are expressed in axons of cerebellar interneurons (Southan et al., 2000); currents through these channels (I_h) can affect axonal length constant near the resting potential (Mejia-Gervacio and Marty, 2006). In voltage clamped mature SCs (−60 mV), we observed that the I_h blocker ZD 7288 (20 μM) did not affect holding current (control, −18.1 ± 2.6 pA; ZD 7288, −19.6 ± 3.9 pA; p > 0.05; paired t-test), a result consistent with earlier work in less mature SCs (Mejia-Gervacio and Marty, 2006). However, the voltage threshold for AP initiation was reduced in mature SCs following I_h block (Supplemental Figure 3) suggestive of a localized effect on membrane potential at the AIS where spikes originate. To evaluate a role for I_h currents in dampening the spread of somatic depolarization in mature animals, we applied ZD 7288 and found that the amplitude of axonal subthreshold potentials were larger and similar to that of juveniles (Figure 7A and 7B) indicating an age-related increase in I_h dependent axonal shunting. In following, we recovered depolarization-induced spike broadening in mature animals in the presence of ZD 7288 (Figure 7C and 7D) indicating that I_h current prohibits subthreshold-induced AP broadening in mature animals. Thus, spike plasticity can be tuned by the active features within the axon to regulate axosomatic integration of subthreshold activity.

Discussion

We find that somatic subthreshold depolarization spreads throughout a large extent of the SC axonal arbor in juvenile mice. At release sites, this depolarization rapidly inactivates $K_v3.4$ subunit-containing channels resulting in a short-term reduction in the availability of K_v3-mediated current. Because AP duration is determined by the K^+ conductance local to a bouton, APs at release sites preceded by subthreshold activity are broader and result in increased spike-evoked Ca^{2+} entry and a greater amount of transmitter release. Analog facilitation is subject to regulation by I_h currents that filter voltage spread in the axon, and competes with synaptic depression (uncovered in the absence of spike-width plasticity) to determine the net effect on neurotransmission. Thus, in young SCs, the combination of strongly spreading subthreshold depolarization with fast-inactivating presynaptic K_v3 channels drives a rapid form of analog-to-digital plasticity at sites of release.

Spread of subthreshold depolarization in axons of cerebellar SCs

Our results show that SC axons are electronically coupled to the soma similar to other neuron types in hippocampus and neocortex (Alle and Geiger, 2006; Foust et al., 2011; Shu et al., 2006). As the SC axon arbor is quite compact (de San Martin et al., 2015), somatic depolarization will spread through a substantial portion of the axon reaching a majority of presynaptic sites before full attenuation. We did not analyze voltage spread under passive conditions. Nonetheless spread of a brief depolarization into the SC axon was in line with the predicted length constant for a passive DC signal (Johnston and Wu, 1995) given realistic SC axon geometry and membrane properties (Abrahamsson et al., 2012; Rowan et

al., 2014). This is surprising, as SC axons express low-voltage activating K^+ channels (Rowan et al. 2016) which can truncate the spread of subthreshold depolarization in axons (Apostolides et al., 2016). Similar to dendrites of neocortical pyramidal neurons (Schwindt and Crill, 1995), SCs express a persistent Na_v conductance (Mann-Metzer and Yarom, 2002) that may counterbalance this effect, helping boost the spread of somatic depolarization throughout the axonal arbor (de San Martin et al., 2015). However, spread of subthreshold depolarization is unaffected by Na_v block in hippocampal granule cells (Alle and Geiger, 2006) indicating that analog signaling is passive in other cell types.

Interestingly, relative to juvenile animals, we find that axosomatic coupling in SCs is reduced in the maturing cerebellum. Axonal dampening manifests as a function of axonal HCN channel activity reducing the spread of somatic excitability into the axon. Similarly, an active K^+ conductance limits the passage of somatic depolarization into axons of CA1 pyramidal cells (Apostolides et al., 2016). The exact mechanism underlying the increase in HCN influence in SCs is unclear but could involve changes in conductance density by developmental regulation of channel expression density, or enhancement of its conductance through cyclic nucleotide signaling (Beaumont and Zucker, 2000; Ingram and Williams, 1996) as HCN channels are already expressed in SC axons in juvenile animals but, interestingly, have little effect on the somatic membrane conductance (Mejia-Gervacio and Marty, 2006). Similarly, we found I_h currents do not contribute to somatic resting membrane potential in mature SCs in contrast to other interneuron types (Maccaferri and McBain, 1996) though these currents can affect membrane potential locally at axonal locations (Kim et al., 2007; Southan et al., 2000). In keeping with this possibility, we observed an effect of HCN channels on AP threshold suggesting a localized role in the proximal SC axon, expressed near the site of spike initiation, similar to that observed in the principal neurons of the auditory brainstem (Ko et al., 2016). Previous investigations have shown that significant alternations in intrinsic neuronal excitability occur during early postnatal development (Desai et al., 1999; Leao et al., 2005; Moody and Bosma, 2005), during aging (Huguenard et al., 1988; Kaczorowski and Disterhoft, 2009), and following learning (Schreurs et al., 1998; Sehgal et al., 2013). Thus, in axons, active membrane properties combine with passive features to endow unique axosomatic coupling properties that are subject to change depending on cell type, age and experience.

Spike plasticity in SC boutons depends on inactivating K_v3 channels

Our measurements in SCs revealed that APs broaden at release sites following brief, subthreshold depolarization. This short-term plastic alteration of AP duration depends on $K_v3.4$ subunit-containing K_v3 channels. Currents mediated by K_v3 channels are known to be strongly recruited during AP repolarization and therefore are the predominant K^+ conductance setting spike width in many axons (Alle et al., 2011; Ishikawa et al., 2003), including SCs, where their variable expression density contributes to near synapse-by-synapse differences in AP duration (Alle et al., 2011; Ishikawa et al., 2003; Rowan et al., 2016). Importantly, K_v3 channels can regulate their availability through rapid open-state, N-type inactivation when incorporating $K_v3.4$ subunits (Fineberg et al., 2012; Rudy and McBain, 2001) and $K_v3.4$ subunit-containing channels have a hyperpolarized activation range (Baranauskas et al., 2003) making them particularly amenable to use-dependent

inactivation by subthreshold potentials. $K_v3.4$ channels recover from inactivation on the order of hundreds of ms to several seconds depending on voltage and the phosphorylation state of the channel (Beck et al., 1998; Ritter et al., 2012). This time course is in line with the short-lived effect of AP broadening after brief depolarizations at SC boutons. It follows that in $K_v3.4^{-/-}$ mice, we find that inactivating K_v3 currents are absent in SC boutons and depolarization-induced AP broadening is abolished, strongly implicating these subunits in spike plasticity. Notably, the involvement of K_v3-mediated currents in use-dependent spike plasticity has not previously been reported and may relate to the distribution pattern of $K_v3.4$ in the CNS. $K_v3.1$ subunits are also constituent components of K_v3 channels in SC axons (Rowan et al., 2016) but are resistant to N-type inactivation (Rudy and McBain, 2001). Therefore, depolarization-induced spike broadening at individual boutons will depend on both the amplitude and duration of the subthreshold potential and the variable composition and expression density of K_v3 channels at each presynaptic location. In contrast to AP duration, we report that analog depolarization does not affect the amplitude of single APs pointing to the absence of an effect on Na_v channels. However, a reserve of Na_v channels may protect the amplitude of individual spikes. SCs fire repetitively at high frequencies like many other interneuron types (Lien and Jonas, 2003; Rudy and McBain, 2001). Therefore, if subthreshold depolarization is sufficient to inactivate some axonal Na_v channels in SCs, a reduction in AP amplitude is plausible during repetitive firing if a Na_v reserve is required to maintain maximal rates of AP output (Madeja, 2000).

Similar to dendrites (Sjostrom et al., 2008), axons increase their computational capability through heterogeneous compartmentalization of their active properties (Debanne et al., 2011). Axons not only transmit but also transform electrical information dependent on previous or ongoing activity (Sasaki, 2013). Here, we report that rapid spike plasticity induced by somatic subthreshold depolarization appears specific to boutons in SCs. This is a likely consequence of the preferential localization of K_v3 channels at release sites. In contrast to boutons, AP repolarization is determined by K_v1-mediated currents in the AIS of SCs rather than K_v3 (Rowan et al., 2014) and is resistant to rapid depolarization-induced spike broadening. Like the AIS of pyramidal cells in the neocortex where K_v1 inactivation underlies spike broadening (Kole et al., 2007), the SC AIS may require prolonged depolarization (e.g., >5 s) to induced spike plasticity however we did not investigate this possibility. In contrast, APs are progressively prolonged in the SC AIS during repetitive spiking in a K_v1-dependent manner, presumably due to accumulating inactivation as observed in mossy fiber boutons of the hippocampus (Geiger and Jonas, 2000; Rowan et al., 2014). Conversely, at SC boutons, APs are resistant to spike-dependent broadening during the same repetitive stimuli due to the predominance of a K_v3 conductance (Rowan et al., 2014). Therefore, the distribution as well as the unique biophysical properties of K_v1 and K_v3 channels at the AIS and boutons of SCs, including voltage-dependent inactivation and deactivation, equip these subcompartments with distinct modalities of plasticity to independently tune spike duration dependent on the specific type of preceding activity. Furthermore, the unique biophysical features of K_v3 channels at SC release sites, namely the inclusion of rapidly-inactivating $K_v3.4$ subunits, confers a fast form of depolarization-induced spike plasticity unlike that of neocortical and hippocampal excitatory cells (Bialowas et al., 2015; Shu et al., 2006; Zhu et al., 2011).

Analog modulation of release in SC axons

Short-term facilitation of release occurs following subthreshold depolarization at many presynaptic specializations (Alle and Geiger, 2006; Awatramani et al., 2005). At the small *en passant* boutons of SCs, we show that presynaptic AP broadening following depolarization results in an increase in spike-evoked Ca^{2+} entry. Previous recordings from 'giant' calyceal terminals and mossy fiber boutons show a linear correlation between AP width and the resultant Ca^{2+} current integral (Bischofberger et al., 2002; Borst and Sakmann, 1999). Depolarization-induced prolongation of AP width results in a similar linear increase in Ca^{2+} influx in SCs. Thus, increases in AP-evoked Ca^{2+} entry following spike broadening must strongly contribute to the analog facilitation at SC boutons as evidenced by the absence of release strengthening in mutant mice lacking $K_v3.4$ inactivation and spike-width plasticity.

Subthreshold depolarization also directly opens voltage-gated Ca^{2+} channels increasing residual Ca^{2+} levels at the release sites of cerebellar molecular layer interneurons (Bouhours et al., 2011; Christie et al., 2011; Pugh and Jahr, 2011). Although analog facilitation has been attributed to PKC activity induced by this residual Ca^{2+} transient (Bouhours et al., 2011), genetic deletion of all Ca^{2+}-dependent PKC isoforms had no effect on depolarization-induced release strengthening. Moreover, in the absence of $K_v3.4$-dependent spike broadening, somatic depolarization results in synaptic depression. Synaptic depression has been linked to an activity-dependent reduction in AP amplitude at the terminal release sites of cerebellar Purkinje cells (Kawaguchi and Sakaba, 2015). However, in SCs, spike amplitude was not significantly reduced by somatic depolarization and analog depression was closely correlated with release probability arguing against this possibility. Because elevation of residual Ca^{2+} during subthreshold depolarization can drive asynchronous neurotransmission (Christie et al., 2011; Christie and Jahr, 2008; Glitsch and Marty, 1999), analog depression may be best explained by depletion of vesicles from the readily releasable pool. Therefore, the effect of somatic depolarization on the strength of neurotransmission will likely depend on the interplay between Ca^{2+}-dependent enhancement of release during AP broadening and the synaptic weakening through a reduction in vesicle pool size.

Experimental Procedures

Experimental Procedures are described in detail in the Supplemental Experimental Procedures. All animal procedures were approved by the Max Planck Florida Institute for Neuroscience Animal Care and Use Committee.

Acute slice preparation

All experiments were performed on acute cerebellar slices prepared from juvenile or mature mice (postnatal day [PND]15–21 or   42, respectively). Brain slices (200 μm) were sectioned in the parasagittal plane using a vibrating blade microtome in an ice cold sucrose-based cutting solution and immediately incubated at 34°C for 30 min and then at room temperature (RT; 23–25°C) in normal ACSF thereafter.

Voltage imaging from SC Axons

The voltage-sensitive dye di-2-AN-(F)EPPTEA (30 mM; L. Loew; University of Connecticut Health Center) was included in the intracellular solution and allowed to diffuse throughout the SC axon for 0.5 hours. Voltage imaging was performed with non-scanning two-photon illumination from single diffraction-limited points on the axon. All imaging was performed with a two-photon laser scanning microscope (Ultima; Bruker Corp.) with excitation provided by a mode-locking Ti:sapphire laser (Chameleon Ultra II; Coherent Inc.) at 1020–1040 nm.

Bouton patch clamp in SC axons

Tight-seal presynaptic channel recordings in SCs were performed under continuous two-photon laser scanning imaging to guide fluorescently labeled pipettes to identified axonal sites of interest after volume dye filling through a somatic recording electrode. K_v3 channel currents were pharmacologically isolated using a patch pipette solution including blockers for Na_v, HCN, K_v7, and K_v1 channels.

Supplementary Material

Refer to Web version on PubMed Central for supplementary material.

Acknowledgments

References

Abbott LF, Regehr WG. Synaptic computation. Nature. 2004; 431:796–803. [PubMed: 15483601]

Abrahamsson T, Cathala L, Matsui K, Shigemoto R, DiGregorio DA. Thin dendrites of cerebellar interneurons confer sublinear synaptic integration and a gradient of short-term plasticity. Neuron. 2012; 73:1159–1172. [PubMed: 22445343]

Acker CD, Yan P, Loew LM. Single-voxel recording of voltage transients in dendritic spines. Biophysical journal. 2011; 101:L11–L13. [PubMed: 21767473]

Alle H, Geiger JR. Combined analog and action potential coding in hippocampal mossy fibers. Science (New York, NY). 2006; 311:1290–1293.

Alle H, Kubota H, Geiger JR. Sparse but highly efficient Kv3 outpace BKCa channels in action potential repolarization at hippocampal mossy fiber boutons. The Journal of neuroscience : the official journal of the Society for Neuroscience. 2011; 31:8001–8012. [PubMed: 21632922]

Apostolides PF, Milstein AD, Grienberger C, Bittner KC, Magee JC. Axonal Filtering Allows Reliable Output during Dendritic Plateau-Driven Complex Spiking in CA1 Neurons. Neuron. 2016; 89:770–783. [PubMed: 26833135]

Awatramani GB, Price GD, Trussell LO. Modulation of transmitter release by presynaptic resting potential and background calcium levels. Neuron. 2005; 48:109–121. [PubMed: 16202712]

Baranauskas G, Tkatch T, Nagata K, Yeh JZ, Surmeier DJ. Kv3.4 subunits enhance the repolarizing efficiency of Kv3.1 channels in fast-spiking neurons. Nature neuroscience. 2003; 6:258–266. [PubMed: 12592408]

Beaumont V, Zucker RS. Enhancement of synaptic transmission by cyclic AMP modulation of presynaptic Ih channels. Nature neuroscience. 2000; 3:133–141. [PubMed: 10649568]

Beck EJ, Sorensen RG, Slater SJ, Covarrubias M. Interactions between multiple phosphorylation sites in the inactivation particle of a K+ channel. Insights into the molecular mechanism of protein kinase C action. The Journal of general physiology. 1998; 112:71–84. [PubMed: 9649584]

Bialowas A, Rama S, Zbili M, Marra V, Fronzaroli-Molinieres L, Ankri N, Carlier E, Debanne D. Analog modulation of spike-evoked transmission in CA3 circuits is determined by axonal Kv1.1 channels in a time-dependent manner. The European journal of neuroscience. 2015; 41:293–304. [PubMed: 25394682]

Bischofberger J, Geiger JR, Jonas P. Timing and efficacy of Ca2+ channel activation in hippocampal mossy fiber boutons. The Journal of neuroscience : the official journal of the Society for Neuroscience. 2002; 22:10593–10602. [PubMed: 12486151]

Borst JG, Sakmann B. Effect of changes in action potential shape on calcium currents and transmitter release in a calyx-type synapse of the rat auditory brainstem. Philosophical transactions of the Royal Society of London Series B, Biological sciences. 1999; 354:347–355. [PubMed: 10212483]

Bouhours B, Trigo FF, Marty A. Somatic depolarization enhances GABA release in cerebellar interneurons via a calcium/protein kinase C pathway. The Journal of neuroscience : the official journal of the Society for Neuroscience. 2011; 31:5804–5815. [PubMed: 21490222]

Brose N, Rosenmund C. Move over protein kinase C, you've got company: alternative cellular effectors of diacylglycerol and phorbol esters. Journal of cell science. 2002; 115:4399–4411. [PubMed: 12414987]

Christie JM, Chiu DN, Jahr CE. Ca(2+)-dependent enhancement of release by subthreshold somatic depolarization. Nature neuroscience. 2011; 14:62–68. [PubMed: 21170054]

Christie JM, Jahr CE. Dendritic NMDA receptors activate axonal calcium channels. Neuron. 2008; 60:298–307. [PubMed: 18957221]

de San Martin JZ, Jalil A, Trigo FF. Impact of single-site axonal GABAergic synaptic events on cerebellar interneuron activity. The Journal of general physiology. 2015; 146:477–493. [PubMed: 26621773]

Debanne D, Campanac E, Bialowas A, Carlier E, Alcaraz G. Axon physiology. Physiological reviews. 2011; 91:555–602. [PubMed: 21527732]

Desai NS, Rutherford LC, Turrigiano GG. Plasticity in the intrinsic excitability of cortical pyramidal neurons. Nature neuroscience. 1999; 2:515–520. [PubMed: 10448215]

Fineberg JD, Ritter DM, Covarrubias M. Modeling-independent elucidation of inactivation pathways in recombinant and native A-type Kv channels. The Journal of general physiology. 2012; 140:513–527. [PubMed: 23109714]

Fioravante D, Chu Y, Myoga MH, Leitges M, Regehr WG. Calcium-dependent isoforms of protein kinase C mediate posttetanic potentiation at the calyx of Held. Neuron. 2011; 70:1005–1019. [PubMed: 21658591]

Foust AJ, Yu Y, Popovic M, Zecevic D, McCormick DA. Somatic membrane potential and Kv1 channels control spike repolarization in cortical axon collaterals and presynaptic boutons. The Journal of neuroscience : the official journal of the Society for Neuroscience. 2011; 31:15490–15498. [PubMed: 22031895]

Geiger JR, Jonas P. Dynamic control of presynaptic Ca(2+) inflow by fast-inactivating K(+) channels in hippocampal mossy fiber boutons. Neuron. 2000; 28:927–939. [PubMed: 11163277]

Glitsch M, Marty A. Presynaptic effects of NMDA in cerebellar Purkinje cells and interneurons. The Journal of neuroscience : the official journal of the Society for Neuroscience. 1999; 19:511–519. [PubMed: 9880571]

Huguenard JR, Hamill OP, Prince DA. Developmental changes in Na+ conductances in rat neocortical neurons: appearance of a slowly inactivating component. Journal of neurophysiology. 1988; 59:778–795. [PubMed: 2452862]

Ingram SL, Williams JT. Modulation of the hyperpolarization-activated current (Ih) by cyclic nucleotides in guinea-pig primary afferent neurons. The Journal of physiology. 1996; 492(Pt 1): 97–106. [PubMed: 8730586]

Ishikawa T, Nakamura Y, Saitoh N, Li WB, Iwasaki S, Takahashi T. Distinct roles of Kv1 and Kv3 potassium channels at the calyx of Held presynaptic terminal. The Journal of neuroscience : the official journal of the Society for Neuroscience. 2003; 23:10445–10453. [PubMed: 14614103]

Johnston, D., Wu, SM. Foundations of cellular neurophysiology. Cambridge, MA: MIT Press; 1995.

Kaczorowski CC, Disterhoft JF. Memory deficits are associated with impaired ability to modulate neuronal excitability in middle-aged mice. Learning & memory (Cold Spring Harbor, NY). 2009; 16:362–366.

Kim JH, Sizov I, Dobretsov M, von Gersdorff H. Presynaptic Ca2+ buffers control the strength of a fast post-tetanic hyperpolarization mediated by the alpha3 Na(+)/K(+)-ATPase. Nature neuroscience. 2007; 10:196–205. [PubMed: 17220883]

Ko KW, Rasband MN, Meseguer V, Kramer RH, Golding NL. Serotonin modulates spike probability in the axon initial segment through HCN channels. Nature neuroscience. 2016; 19:826–834. [PubMed: 27110919]

Kole MH, Letzkus JJ, Stuart GJ. Axon initial segment Kv1 channels control axonal action potential waveform and synaptic efficacy. Neuron. 2007; 55:633–647. [PubMed: 17698015]

Laube G, Roper J, Pitt JC, Sewing S, Kistner U, Garner CC, Pongs O, Veh RW. Ultrastructural localization of Shaker-related potassium channel subunits and synapse-associated protein 90 to septate-like junctions in rat cerebellar Pinceaux. Brain research Molecular brain research. 1996; 42:51–61. [PubMed: 8915580]

Leao RM, Kushmerick C, Pinaud R, Renden R, Li GL, Taschenberger H, Spirou G, Levinson SR, von Gersdorff H. Presynaptic Na+ channels: locus, development, and recovery from inactivation at a high-fidelity synapse. The Journal of neuroscience : the official journal of the Society for Neuroscience. 2005; 25:3724–3738. [PubMed: 15814803]

Li L, Bischofberger J, Jonas P. Differential gating and recruitment of P/Q-, N-, and R-type Ca2+ channels in hippocampal mossy fiber boutons. The Journal of neuroscience : the official journal of the Society for Neuroscience. 2007; 27:13420–13429. [PubMed: 18057200]

Lien CC, Jonas P. Kv3 potassium conductance is necessary and kinetically optimized for high-frequency action potential generation in hippocampal interneurons. The Journal of neuroscience : the official journal of the Society for Neuroscience. 2003; 23:2058–2068. [PubMed: 12657664]

Maccaferri G, McBain CJ. The hyperpolarization-activated current (Ih) and its contribution to pacemaker activity in rat CA1 hippocampal stratum oriens-alveus interneurones. The Journal of physiology. 1996; 497(Pt 1):119–130. [PubMed: 8951716]

Madeja M. Do neurons have a reserve of sodium channels for the generation of action potentials? A study on acutely isolated CA1 neurons from the guinea-pig hippocampus. The European journal of neuroscience. 2000; 12:1–7. [PubMed: 10651854]

Mann-Metzer P, Yarom Y. Jittery trains induced by synaptic-like currents in cerebellar inhibitory interneurons. Journal of neurophysiology. 2002; 87:149–156. [PubMed: 11784737]

Mejia-Gervacio S, Marty A. Control of interneurone firing pattern by axonal autoreceptors in the juvenile rat cerebellum. The Journal of physiology. 2006; 571:43–55. [PubMed: 16339174]

Moody WJ, Bosma MM. Ion channel development, spontaneous activity, and activity-dependent development in nerve and muscle cells. Physiological reviews. 2005; 85:883–941. [PubMed: 15987798]

Peterka DS, Takahashi H, Yuste R. Imaging voltage in neurons. Neuron. 2011; 69:9–21. [PubMed: 21220095]

Pouzat C, Marty A. Somatic recording of GABAergic autoreceptor current in cerebellar stellate and basket cells. The Journal of neuroscience : the official journal of the Society for Neuroscience. 1999; 19:1675–1690. [PubMed: 10024354]

Pugh JR, Jahr CE. NMDA receptor agonists fail to alter release from cerebellar basket cells. The Journal of neuroscience : the official journal of the Society for Neuroscience. 2011; 31:16550–16555. [PubMed: 22090481]

Rama S, Zbili M, Debanne D. Modulation of spike-evoked synaptic transmission: The role of presynaptic calcium and potassium channels. Biochimica et biophysica acta. 2015; 1853:1933–1939. [PubMed: 25461842]

Ritter DM, Ho C, O'Leary ME, Covarrubias M. Modulation of Kv3.4 channel N-type inactivation by protein kinase C shapes the action potential in dorsal root ganglion neurons. The Journal of physiology. 2012; 590:145–161. [PubMed: 22063632]

Rowan MJ, DelCanto G, Yu JJ, Kamasawa N, Christie JM. Synapse-Level Determination of Action Potential Duration by K(+) Channel Clustering in Axons. Neuron. 2016; 91:370–383. [PubMed: 27346528]

Rowan MJ, Tranquil E, Christie JM. Distinct Kv channel subtypes contribute to differences in spike signaling properties in the axon initial segment and presynaptic boutons of cerebellar interneurons. The Journal of neuroscience : the official journal of the Society for Neuroscience. 2014; 34:6611–6623. [PubMed: 24806686]

Rudy B, McBain CJ. Kv3 channels: voltage-gated K+ channels designed for high-frequency repetitive firing. Trends in neurosciences. 2001; 24:517–526. [PubMed: 11506885]

Sabatini BL, Regehr WG. Timing of neurotransmission at fast synapses in the mammalian brain. Nature. 1996; 384:170–172. [PubMed: 8906792]

Sasaki T. The axon as a unique computational unit in neurons. Neuroscience research. 2013; 75:83–88. [PubMed: 23298528]

Schreurs BG, Gusev PA, Tomsic D, Alkon DL, Shi T. Intracellular correlates of acquisition and long-term memory of classical conditioning in Purkinje cell dendrites in slices of rabbit cerebellar lobule HVI. The Journal of neuroscience : the official journal of the Society for Neuroscience. 1998; 18:5498–5507. [PubMed: 9651230]

Schwindt PC, Crill WE. Amplification of synaptic current by persistent sodium conductance in apical dendrite of neocortical neurons. Journal of neurophysiology. 1995; 74:2220–2224. [PubMed: 8592214]

Sehgal M, Song C, Ehlers VL, Moyer JR Jr. Learning to learn - intrinsic plasticity as a metaplasticity mechanism for memory formation. Neurobiology of learning and memory. 2013; 105:186–199. [PubMed: 23871744]

Shu Y, Hasenstaub A, Duque A, Yu Y, McCormick DA. Modulation of intracortical synaptic potentials by presynaptic somatic membrane potential. Nature. 2006; 441:761–765. [PubMed: 16625207]

Sjostrom PJ, Rancz EA, Roth A, Hausser M. Dendritic excitability and synaptic plasticity. Physiological reviews. 2008; 88:769–840. [PubMed: 18391179]

Southan AP, Morris NP, Stephens GJ, Robertson B. Hyperpolarization-activated currents in presynaptic terminals of mouse cerebellar basket cells. The Journal of physiology 526 Pt. 2000; 1:91–97.

Southan AP, Robertson B. Electrophysiological characterization of voltage-gated K(+) currents in cerebellar basket and purkinje cells: Kv1 and Kv3 channel subfamilies are present in basket cell nerve terminals. The Journal of neuroscience : the official journal of the Society for Neuroscience. 2000; 20:114–122. [PubMed: 10627587]

von Gersdorff H, Borst JG. Short-term plasticity at the calyx of Held. Nature reviews Neuroscience. 2002; 3:53–64. [PubMed: 11823805]

Whim MD, Kaczmarek LK. Heterologous expression of the Kv3.1 potassium channel eliminates spike broadening and the induction of a depolarizing afterpotential in the peptidergic bag cell neurons. The Journal of neuroscience : the official journal of the Society for Neuroscience. 1998; 18:9171–9180. [PubMed: 9801357]

Yeung SY, Thompson D, Wang Z, Fedida D, Robertson B. Modulation of Kv3 subfamily potassium currents by the sea anemone toxin BDS: significance for CNS and biophysical studies. The Journal of neuroscience : the official journal of the Society for Neuroscience. 2005; 25:8735–8745. [PubMed: 16177043]

Zhu J, Jiang M, Yang M, Hou H, Shu Y. Membrane potential-dependent modulation of recurrent inhibition in rat neocortex. PLoS biology. 2011; 9:e1001032. [PubMed: 21445327]

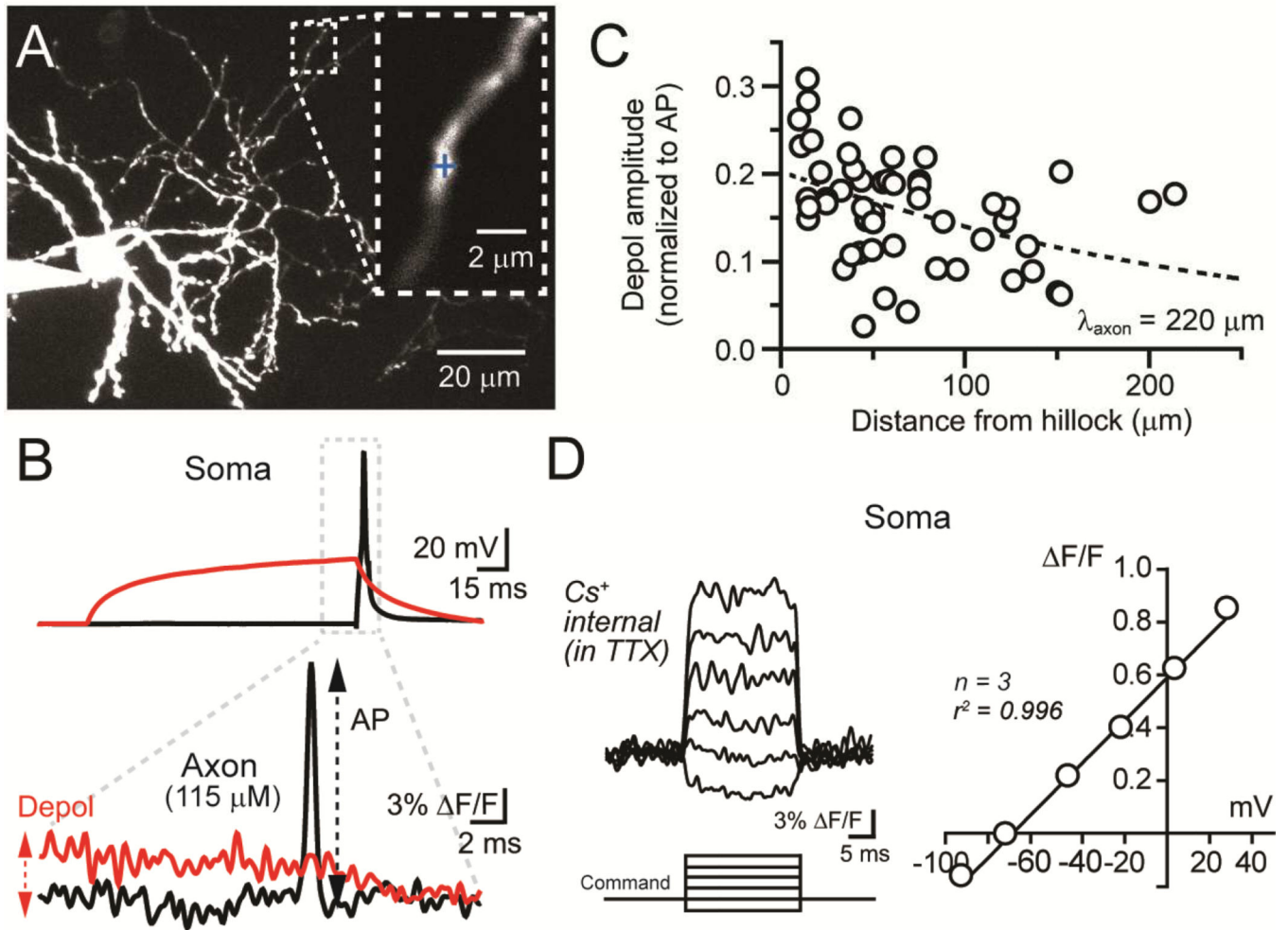Zucker RS, Regehr WG. Short-term synaptic plasticity. Annual review of physiology. 2002; 64:355–405.

Figure 1. Spread of somatic subthreshold depolarization into the axon

(A) 2P maximum intensity image of a SC with a VSD recording site on the axon demarcated in the inset. The cell was filled with the VSD di-2-AN(F)EPPTEA by patch pipette.

(B) A somatically evoked AP or subthreshold depolarization recorded at the soma using electrophysiology and the corresponding voltage response measured at the axon using VSD imaging from the recording site depicted in the image above. Traces are the average of 35 interleaved trials. To infer the amplitude of the subthreshold potential at the axon, the peak VSD fluorescence response induced by the depolarization was compared relative to that of an AP measured at the same location.

(C) The relative amplitudes of somatically-elicited potentials measured along the axon are plotted against the distances of the recording sites from the soma. An exponential fit to the data yielded an estimate of the length constant for spread of subthreshold depolarization into the axon (λ_{axon}). Axonal measurements were grouped from many cells.

(D) VSD measurements from the somatic membrane to a series of voltage steps applied in voltage-clamp mode during whole-cell recording. The change in VSD fluorescence was linearly proportional to the change in membrane potential across a physiologically relevant range.
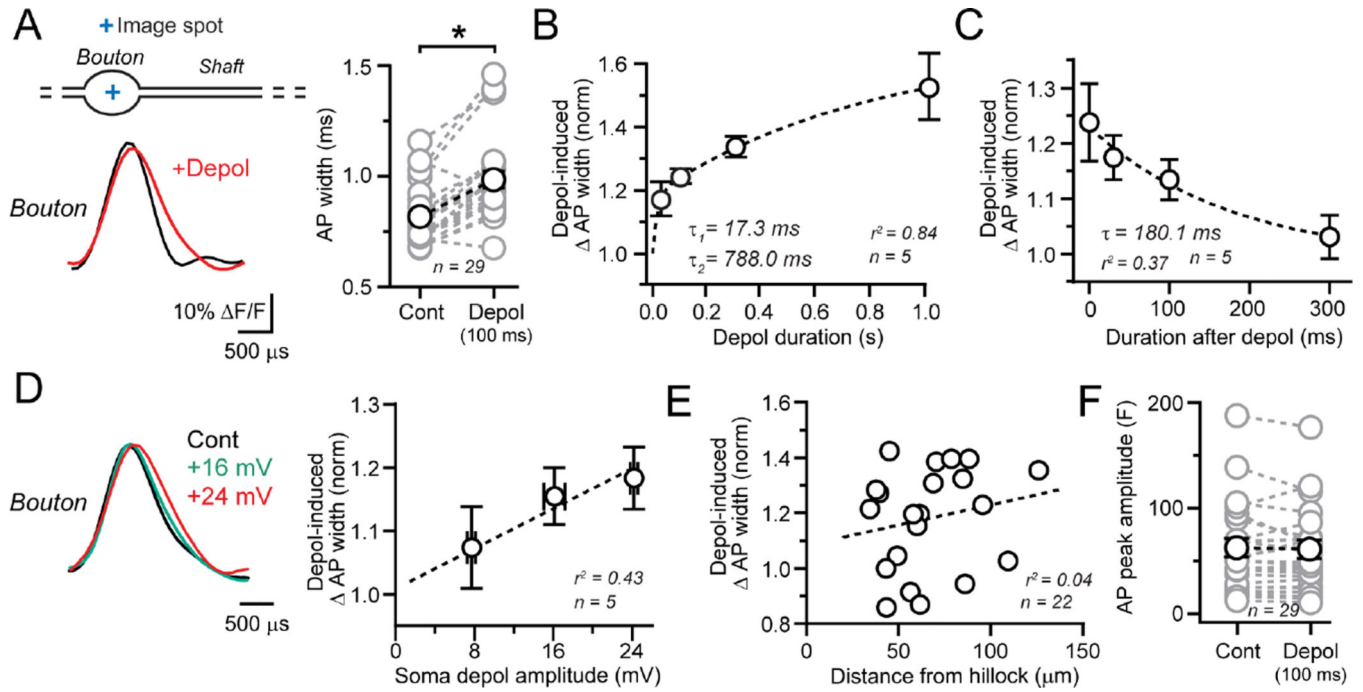
Figure 2. Presynaptic AP broadening induced by somatic depolarization

(A) Somatically-evoked APs measured at an axonal bouton using VSD imaging. In interleaved trials, the spike was immediately preceded by somatic subthreshold depolarization (100 ms, 23.9 ± 4.8 mV at the soma). For the summary plot, mean AP width ($\pm$ SEM) is shown in black and individual bouton measurements in gray (*$p < 0.05$; paired t-test).

(B) The relationship between depolarization-induced AP broadening at boutons and the duration of the preceding somatic subthreshold stimulus was fit with a bi-exponential function.

(C) The decay of depolarization-induced spike broadening (100 ms) at boutons, fit with a mono-exponential function.

(D) APs measured at a bouton using VSD imaging immediately following somatic subthreshold depolarization (100 ms) of varying amplitude. For boutons, the change in AP width induced by somatic depolarization is plotted against the amplitude of the preceding depolarization measured at the soma.

(E) AP broadening induced by somatic depolarization (100 ms) is plotted against the distance of the bouton recording site from the soma. Data are grouped from many cells.

(F) AP amplitude at boutons is unaffected by somatic depolarization ($p > 0.05$; wilcoxon-matched pairs test).
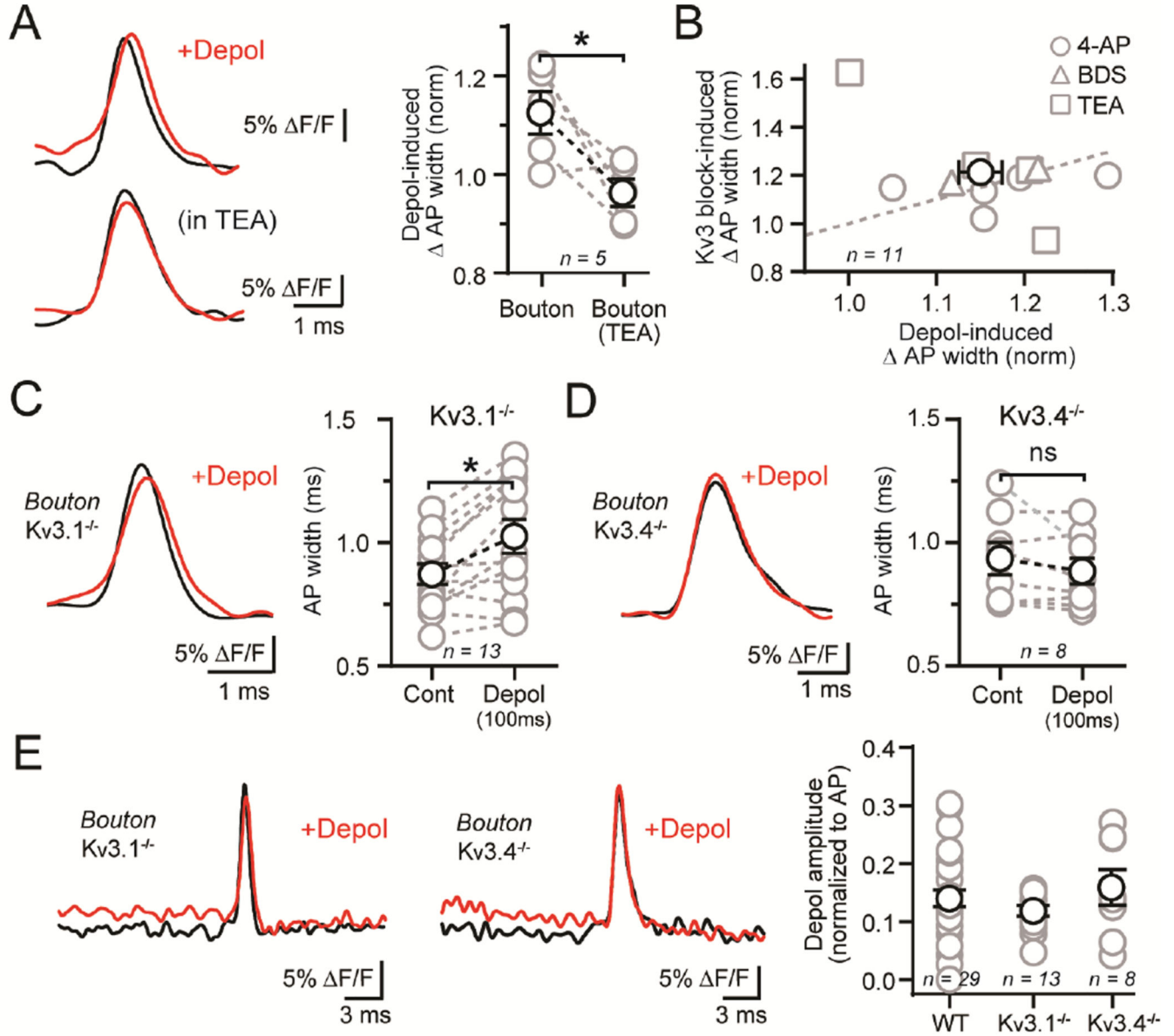
See also Figure S1.

Figure 3. Depolarization-induced AP broadening at boutons requires K_V3 channels

(A) APs paired with or without somatic depolarization measured at a bouton in control (top) or following application of the K_V3 blocker TEA (bottom). The summary plot shows the effect of TEA on depolarization-induced AP broadening. Data are represented as mean (± SEM) with individual data points in gray (*p < 0.05; paired t-test).

(B) For individual boutons, the increase in AP duration induced by somatic depolarization is plotted against the width change induced by K_V3 inhibition at the same site (*circles*, 4-AP [30 µM], n = 4; *triangles*, BDS-1 [1 µM], n = 3; *squares*, TEA [500 µM], n = 5). Dashed line shows unity.

(C) Averaged traces from a VSD bouton recordings in a $K_v3.1^{-/-}$ mouse. In alternating trials, APs were preceded by somatic depolarization. Summary on the right (*p > 0.05; paired t-test).

(D) APs measured in $K_v3.4^{-/-}$ mice prior to and immediately after somatic depolarization. Summary shows the absence of depolarization-induced spike broadening (ns; p > 0.05; paired t-test).

(E) Measurement of subthreshold potentials in the boutons of $K_v3.1^{-/-}$ and $K_v3.4^{-/-}$ mice. On the right, comparison of the effective spread of somatic depolarization in WT and K_v3 subunit KO mice (p > 0.05; 1-way ANOVA with Tukey's multiple comparisons test).
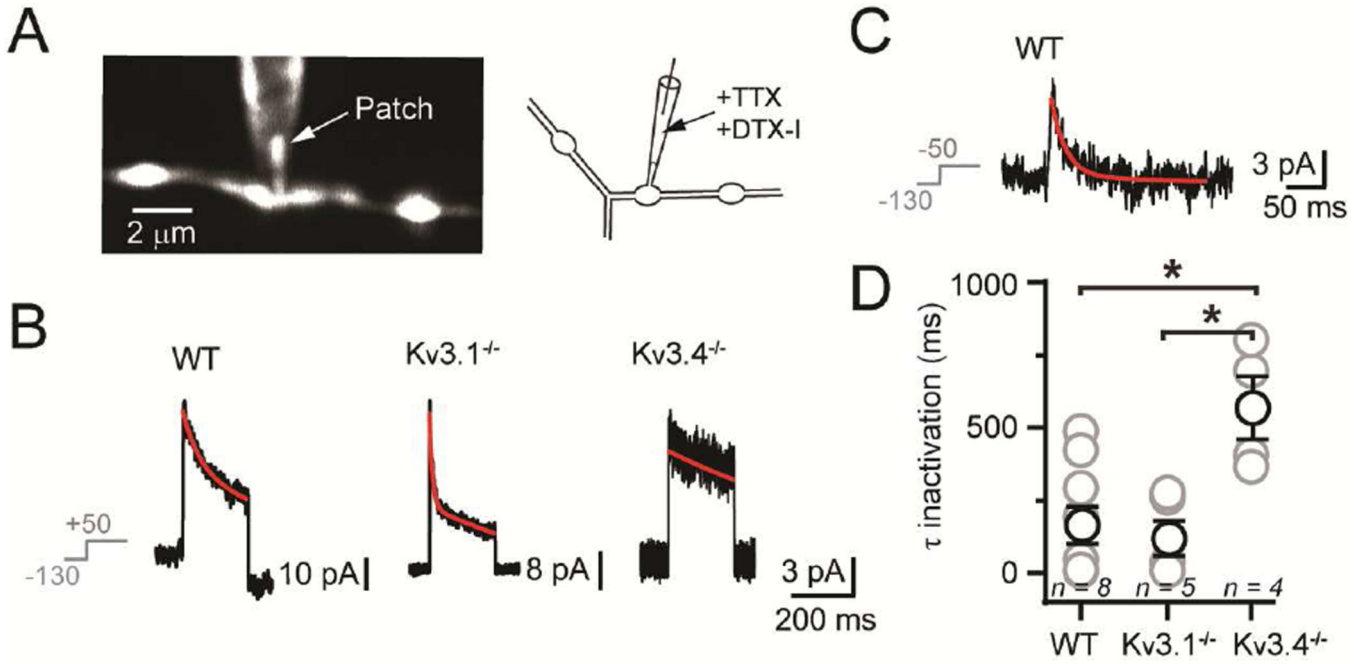
Figure 4. Inactivating K$_v$3 currents in boutons

(A) Axonal patch recording obtained using 2P fluorescence-targeted recording and cartoon depiction of the experimental recording configuration.

(B) Representative K$_v$3 current traces from three bouton recordings for WT, K$_v$3.1$^{-/-}$, and K$_v$3.4$^{-/-}$ mice during a maximally activating depolarizing pulse (+50 mV). An exponential was fit to the current decay for each trace and is shown in red.

(C) K$_v$3 current trace from a WT mouse to a subthreshold depolarizing pulse (−50 mV).

(D) Summary plot of K$_v$3 current weighted decay constants from bouton patches in WT and K$_v$3 KO mice. Significance (*p < 0.05) was determined with 1-way ANOVA with Tukey's multiple comparisons test.
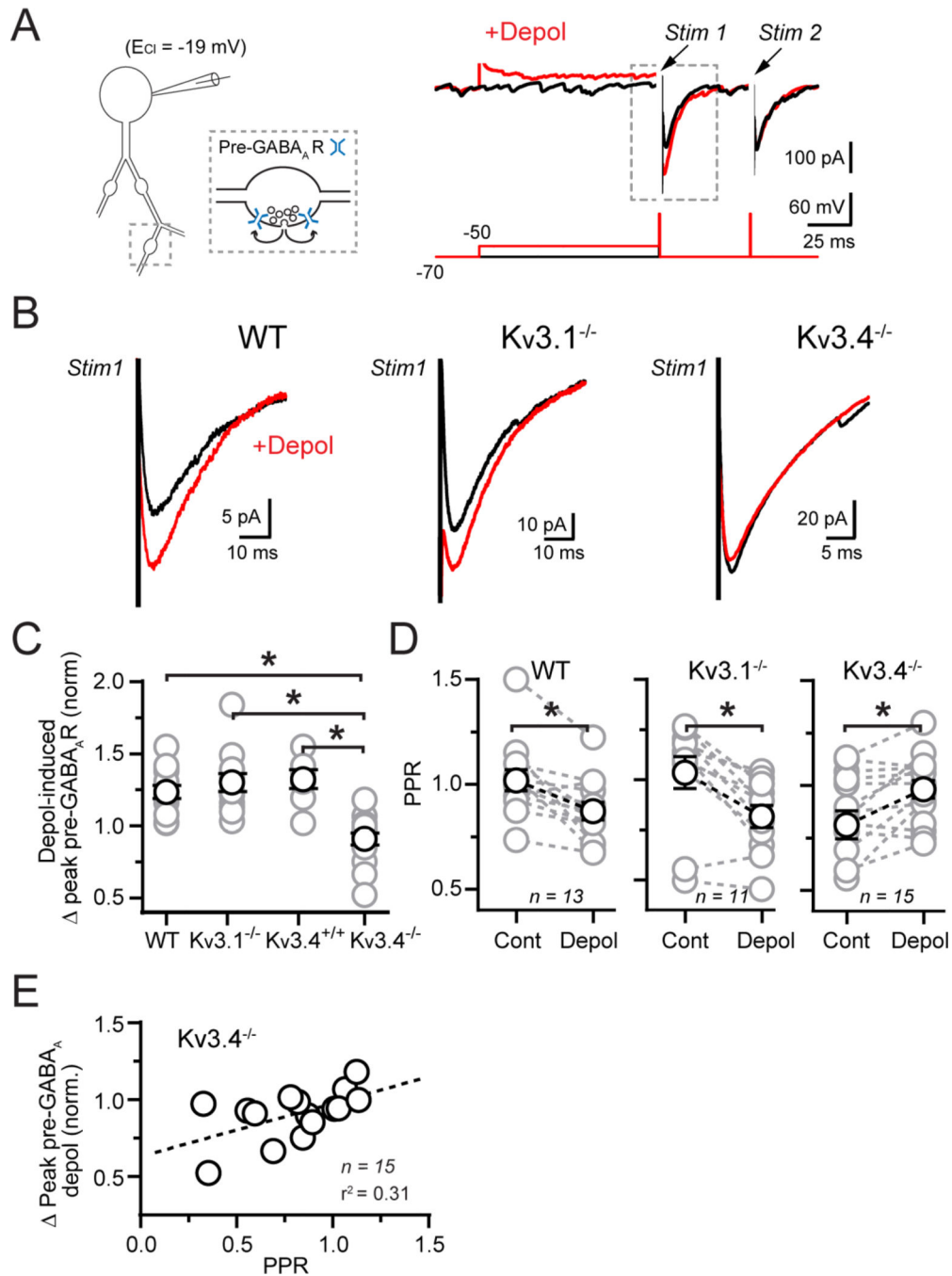
Figure 5. Analog facilitation depends on inactivating K_V3 currents

(**A**) AP-evoked $GABA_A$ autoreceptor currents evoked by unclamped spikes were measured at the soma in interleaved trials either to a spike alone or with a preceding depolarizing pulse (100 ms).

(**B**) Comparison of pre-$GABA_A$R currents in WT and K_v3 subunit KO mice.

(**C**) Summary plot showing the effect of somatic depolarization on synaptic efficacy in K_v3 subunit KO mice. Mean data ±SEM are in black with individual data points in gray.

Significance (*p < 0.05) was determined with 1-way ANOVA with Tukey's multiple comparisons test.

(D) Depolarization-induced changes in PPR (inter-stimulus interval, 50 ms) of spike-evoked pre-GABA$_A$R currents.

(E) Relationship between basal PPR and depolarization-induced synaptic weakening in K$_v$3.4 KO mice.
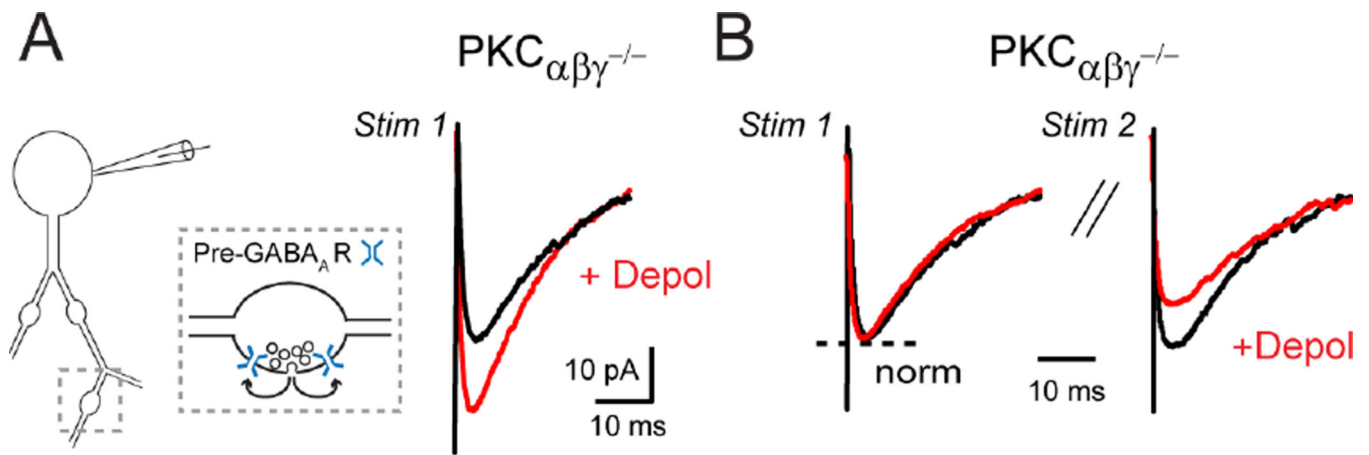
See also Figure S2.

Figure 6. Analog facilitation in mice lacking Ca^{2+}-dependent PKC isoforms
(A) Pre-GABA$_A$R currents in PKC$_{\alpha\beta\gamma}^{-/-}$ mice evoked by unclamped spikes preceded by somatic depolarization.

(B) Responses to paired pulse stimulation from the same neuron are shown normalized to the peak of the first response.
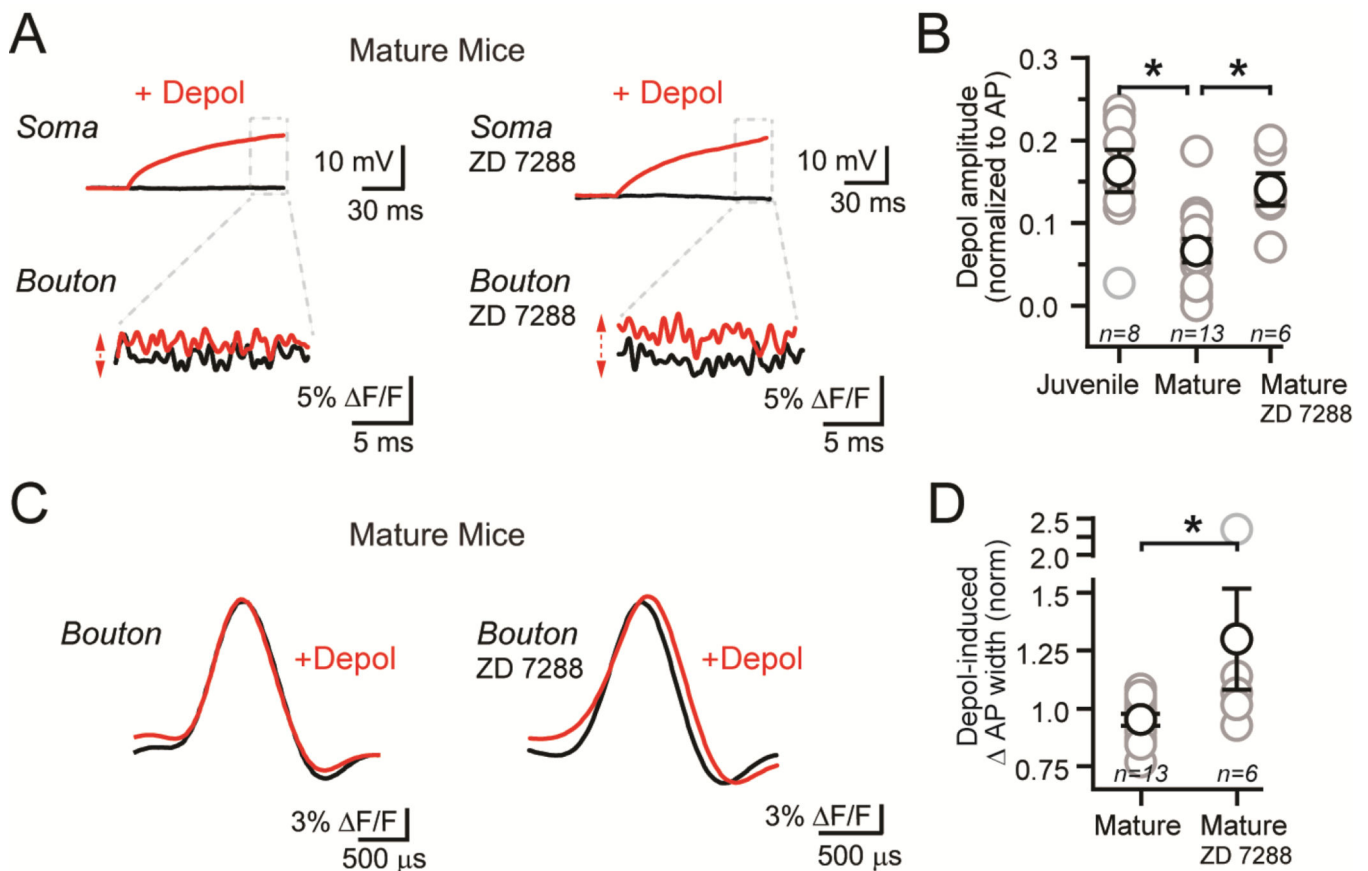
Figure 7. Developmental regulation of subthreshold voltage signaling in axons

(A) In mature mice (PND 42), measurement of subthreshold potentials in boutons evoked by somatic depolarization in control and after bath application of the HCN blocker ZD 7288 (20 μM).

(B) Summary plot of the relative amplitudes of subthreshold potentials at two developmental stages (PND 15–21 and PND 42). All recording sites were <100 μm from the soma. Mean data ±SEM shown in black with significance (*p > 0.05) determined by 1-way ANOVA followed by Tukey's multiple comparisons test. Somatic depolarization; juvenile, 24.7 ± 2.9 mV, n = 8; mature, 22.1 ± 2.1 mV, n = 13 (p > 0.05; unpaired t-test).

(C) APs with and without preceding somatic depolarization measured at two different boutons in mature mice: on the left, in control conditions and, on the right, with the HCN channel blocker ZD 7288.

(D) Plot showing the change in AP width following subthreshold depolarization in mature animals (> PND 42) in control and with the HCN blocker ZD 7288. All recordings were performed at 32°C in this figure.

See also Figure S3.